NANO LETTERS

Letter

pubs.acs.org/NanoLett

Morphology and Thermodynamic Properties of a Copolymer with an Electronically Conducting Block: Poly(3-ethylhexylthiophene)-*block*-poly(ethylene oxide)

Shrayesh N. Patel,[†,‡,⊥] Anna E. Javier,[†,§,⊥] Keith M. Beers,[†,‡] John A. Pople,[∥] Victor Ho,[†,‡] Rachel A. Segalman,[†,‡] and Nitash P. Balsara*[,†,‡,§]

[†]Department of Chemical and Biomolecular Engineering, University of California, Berkeley, Berkeley, California 94720, United States

[‡]Materials Sciences Division, Lawrence Berkeley National Laboratory, Berkeley, California 94720, United States

[§]Environmental Energy Technologies Division, Lawrence Berkeley National Laboratory, Berkeley, California 94720, United States

[∥]Stanford Synchrotron Radiation Laboratory, SLAC National Accelerator Laboratory, Stanford, California 94309, United States

Supporting Information

ABSTRACT: We report on the synthesis and morphology of a block copolymer, poly(3-(2′-ethylhexyl)thiophene)-*b*-poly(ethylene oxide) (P3EHT-*b*-PEO), that conducts both electrons and ions. We show that in the melt state the P3EHT-*b*-PEO chains self-assemble to produce traditional nanoscale morphologies such as lamellae and gyroid. This is in contrast to a majority of previous studies on copolymers with electronically conducting blocks wherein a nanofibrillar morphology is obtained. Our approach enables estimation of the Flory–Huggins interaction parameter, χ. The segregation strength between the two blocks is controlled through the addition of lithium bis(trifluoromethanesulfonyl)imide (LiTFSI). For the salt-free sample, the gyroid morphology, obtained in the melt state, is transformed into lamellae below the melting temperature of the P3EHT block. This is due to the "breaking out" of the crystalline phase. For the salt-containing sample, P3EHT-*b*-PEO has a lamellar morphology in both melt and crystalline states (confined crystallization).

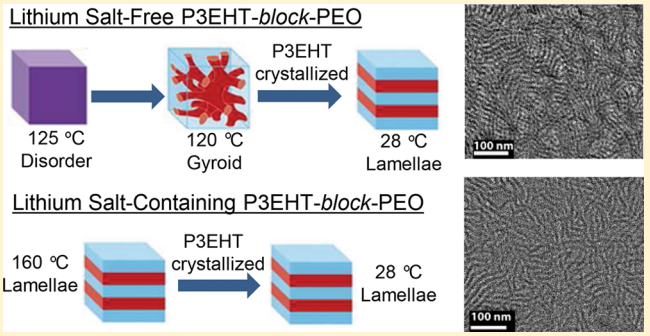

KEYWORDS: *Conducting polymers, semicrystalline block copolymer, order-to-disorder transition, confined crystallization, breakout crystallization*

Nanostructuring of electronically conducting domains is important for a wide range of applications related to clean energy. Organic solar cells require nanoscale electron- and hole-conducting domains to promote charge separation and extraction.[1] Battery and fuel cell electrodes based on active materials that are either electronic or ionic insulators (e.g., lithium iron phosphate or platinum) require nanoscale electron- and ion-conducting domains.[2,3] Copolymers with electronically conducting block such as poly(3-alkylthiophenes) (P3AT) appear to be perfectly suited for such applications.[4] It is thus not surprising that many research groups have focused on the synthesis and characterization of block copolymers containing P3AT.[5−8] The formation of nanoscale domains such as alternating lamellae and the cubic gyroid phase in block copolymers[9] is well established, and such morphologies are ideally suited for the applications listed above. Unfortunately, the crystallization of most electronically conducting polymers disrupts these morphologies; a vast majority of publications on P3AT report the formation of crystalline nanofibrils with no evidence of conventional domain morphologies seen in block copolymers.[5−8] Notable exceptions are the reports from Ho et al.[10] and Moon et al.,[11] who report the formation of conventional morphologies in a P3AT-containing block copolymers that have reduced melting temperatures. The common feature in these studies is that the nonconducting blocks have a high glass transition temperature, and the inability of glassy polymers to conduct either electrons or ions is well established.

This paper demonstrates the formation of lamellae and gyroid morphologies in a poly(3-(2′-ethylhexyl)thiophene)-*b*-poly(ethylene oxide) (P3EHT-*b*-PEO) copolymer. The P3EHT block has a molecular weight of 5 kg/mol, and the PEO block has a molecular weight of 2 kg/mol (we see no evidence of PEO crystals in our experimental window). We also show that the morphology is affected by the addition of lithium bis(trifluoromethanesulfonyl)imide (LiTFSI), a salt that is commonly used in the field of polymer electrolytes. We provide thermodynamic data that represent the starting point for predicting the morphologies of these systems. The distinguish-

Received: July 2, 2012
Revised: July 25, 2012
Published: July 27, 2012

   dx.doi.org/10.1021/nl302454c | *Nano Lett.* 2012, 12, 4901−4906

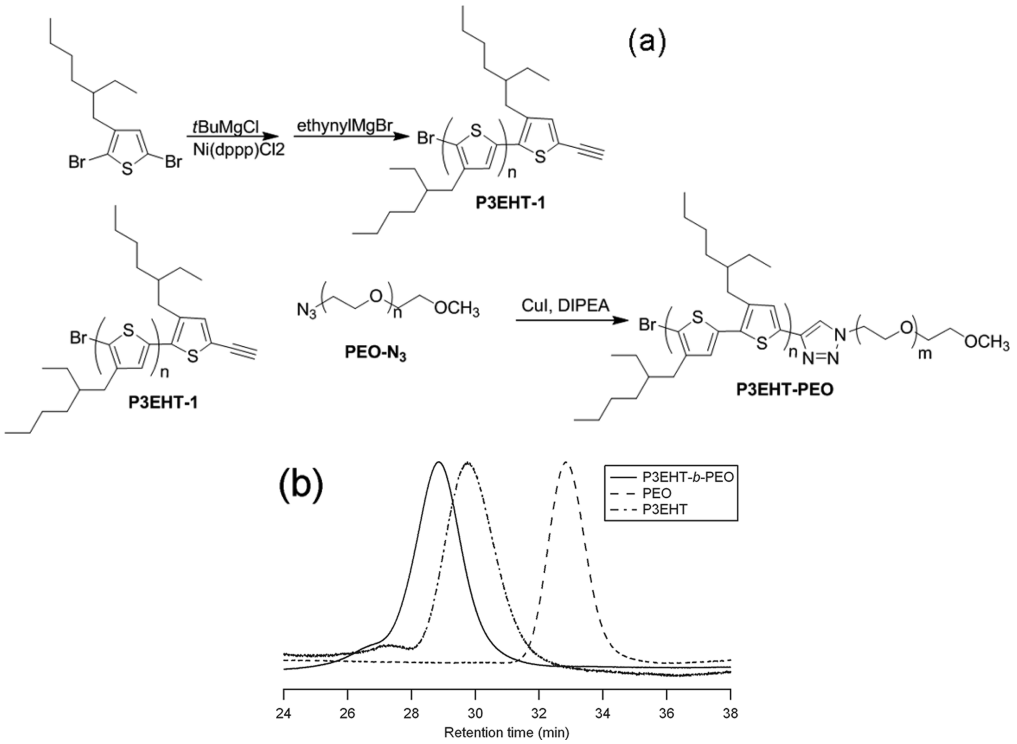

Figure 1. (a) Synthetic scheme of P3EHT-*b*-PEO block copolymer. (b) SEC traces of homopolymers and P3EHT-*b*-PEO (see Supporting Information for more details).

ing feature of our study is the rubbery nature of PEO-rich microphases which enables ion transport, thus allowing for simultaneous conduction of electronic and ionic charges.

A framework has been established to predict the self-assembly of copolymers with one nonconducting crystallizable block and one amorphous block.[12−21] The morphology obtained in these systems is dictated by the chemical incompatibility of the two blocks (χ, Flory−Huggins interaction parameter), the free energy of crystallization, and the glass transition temperature of the amorphous block.[12−21] When the amorphous block is glassy, the morphology of the melt state is retained and the crystallization of the second block is confined within the nanoscale domains.[14,16,19,22] When the amorphous block is rubbery, the morphology in the crystalline state depends on both segregation strength (χN, where N is the number of monomers per chain) between the blocks and the free energy of crystallization.[12,14,16,18] The melt-state morphology is retained only in strongly segregated systems.[16−18] In weakly segregated systems, the crystalline phase "breaks out" of the confining block copolymer domain.[12−14,18,20,21] The breakout morphology of the crystalline phase is often lamellar as this geometry is commensurate with that of chain folded crystals.[12,14,21,23,24] This was first anticipated by theorists[23,24] and subsequently observed experimentally.[12−14,21] The thermodynamic properties of our P3EHT-*b*-PEO block copolymer are consistent with this general framework.

Poly(3-hexylthiophene) (P3HT) is a highly studied semicrystalline polymer system due to its high electronic charge carrier mobility.[25,26] P3HT has a high melting temperature (<230 °C) and is dominated by crystallization through strong $\pi-\pi$ interactions. As a result, the morphology of P3HT-containing block copolymers have nanofibrillar superstructure.[5−8] Variations in the alkyl side chain of the thiophene block can have a large effect on the crystalline and liquid crystalline properties of P3ATs. For example, poly(3-dodecylthiophene) (P3DDT) has a lower melting point (160 °C) and reduced rod−rod interactions relative to P3HT.[27] Moon et al. show that one can obtain traditional block copolymer morphologies with P3DDT-*b*-poly(methyl methacrylate) (P3DDT-*b*-PMMA) by varying the molecular weight of P3DDT and PMMA, thus controlling the segregation strength.[11] The nanofibril morphology is only obtained when the total molecular weight is reduced and P3DDT is the majority block. Importantly, the crystalline nature of P3DDT is retained in the nanoscale domains for the whole composition window.

In addition to P3HT and P3DDT, the introduction of a branched alkyl side chain, such as in poly(3-(2′-ethylhexyl)-thiophene) (P3EHT), causes the polymer to have an even lower melting temperature (80 °C) and reduced rod−rod interactions.[27] The P3EHT homopolymers and P3EHT-containing block copolymers[10] have been shown to crystallize similarly to P3HT by forming the $\pi-\pi$ stacked polymer chains[27] and also has comparable optical and charge transport properties to those of P3HT.[10,27,28] The use of a P3AT derivative with a lowered crystallization temperature can affect the self-assembly of P3EHT rod−coil block copolymers. Ho et al. have observed traditional block copolymer morphologies with a P3EHT-*b*-polylactide (P3EHT-*b*-PLA) system.[10] This result is consistent with the framework described above; confined crystallization can be attributed to the low crystallization temperature of P3EHT, the glassy nature of the noncrystalline block, and the strong segregation strength between the two blocks.

We present a facile approach for synthesizing P3EHT-*b*-PEO copolymers that combines Grignard metathesis (GRIM) polymerization and click chemistry (Figure 1a).[29] An ethynyl-terminated P3EHT homopolymer was first synthesized

dx.doi.org/10.1021/nl302454c | *Nano Lett.* 2012, 12, 4901−4906

followed by coupling with an azide-terminated PEO homopolymer. Matrix-assisted laser desorption ionization time-of-flight mass spectrometry (MALDI-TOF MS) was employed to determine the end-group composition of the end-capped P3EHT, and a representative spectrum is shown in the Supporting Information. To our knowledge, this is the first time that the end-capping methodology with the GRIM mechanism has been used for P3EHT block copolymer synthesis. Figure 1b shows the size exclusion chromatography (SEC) traces of the two homopolymers and the block copolymer. The formation of the block copolymer is evidenced by the difference in elution volume between the P3EHT homopolymer and the P3EHT-*b*-PEO copolymer traces (see Supporting Information for more details). This is further confirmed by ^{1}H nuclear magnetic resonance (^{1}H NMR) spectroscopy, which shows the disappearance of the ethynyl proton peak (see Supporting Information).

Figure 2a shows differential scanning calorimetry (DSC) data for neat P3EHT-*b*-PEO (r = 0, where r is the molar ratio of Li^+

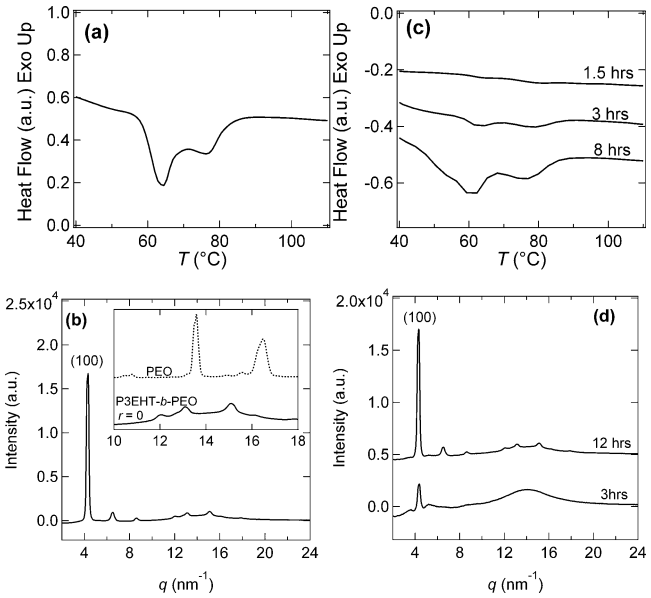

Figure 2. (a) DSC heating scan of P3EHT-*b*-PEO (r = 0) at 10 °C/min after an isothermal wait step of 1.5 h at 30 °C; (b) WAXS curve of P3EHT-*b*-PEO (r = 0) where the inset compares WAXS curves of PEO homopolymer (dotted curve) and P3EHT-*b*-PEO (r = 0) (solid curve); (c) DSC heating scans of P3EHT-*b*-PEO (r = 0.125) at 10 °C/min after an isothermal wait step of 1.5, 3, and 8 h at 30 °C; (d) WAXS curves of P3EHT-*b*-PEO (r = 0.125) after going above the melting temperature, cooling to 30 °C and waiting for 3 and 12 h. The P3EHT block for both r = 0 and r = 0.125 remain semicrystalline as indicated by the melting peaks in the DSC scans and the (100) reflection in the WAXS profiles. PEO block does not crystallize within our experimental window as indicated by the lack of WAXS peaks corresponding to PEO crystallites (inset of part b). The P3EHT block for the r = 0 sample crystallized in 1.5 h, while the r = 0.125 showed a very weak melting peak in 1.5 h. However, a more pronounced P3EHT melting peak was observed after 8 h.

to ethylene oxide monomer). The neat sample was held at 30 °C for 90 min prior to heating to allow for the complete crystallization of the P3EHT block. Melting peaks at 64 and 77 °C are observed, consistent with previous reports.[28] PEO chains in the P3EHT-*b*-PEO do not crystallize in the temperature window of interest, 25−160 °C. Consequently, no melting peak for PEO is observed in Figure 2a (refer to Supporting Information for additional DSC data related to PEO crystallization). Figure 2b shows the wide-angle X-ray scattering (WAXS) for neat P3EHT-*b*-PEO, which was held at 28 °C for 90 min. The resulting scattering peaks are consistent with previously published WAXS data on P3EHT, where the sharp peak at 0.44 nm^{-1} corresponds to the (100) plane (side-chain packing). The scattering peaks for crystalline PEO are not observed, confirming that the P3EHT block is the only crystallized component. The introduction of the LiTFSI salt at a concentration of r = 0.125 leads to much weaker melting peaks in the DSC data (Figure 2c) at 65 and 81 °C. Increasing the isothermal crystallization time from 3 to 8 h results in an increase in intensity of the melting peaks and a small decrease in the melting temperatures to 62 and 76 °C. The longer crystallization time required for the salt-containing sample was further confirmed through WAXS, where the scattering peaks could only be seen after annealing at 28 °C for 12 h (Figure 2d). Both the DSC and WAXS data suggest that the crystallization kinetics of the P3EHT block is affected by the addition of salt. Previous studies on P3HT containing block copolymers indicate some LiTFSI partitions into the P3HT domain.[30] Therefore, it is possible some LiTFSI is partitioning into the P3EHT domain, which could explain different crystallization properties, particularly the slightly lower melting temperature.

Figure 3a shows the small-angle X-ray scattering (SAXS) intensity, I, vs the magnitude of the scattering vector, q, of P3EHT-*b*-PEO for r = 0. At 28 and 50 °C, the scattering profiles indicate two broad shoulders that index to q^* and $2q^*$, where q^* is the magnitude of the scattering vector associated with {100} family of reflection planes of a given morphology. The characteristic domain spacing, $d = 2\pi/q_{max}$, is 15.9 nm, where q_{max} is the magnitude of q at the most intense peak (or the peak that occurs at the lowest value of q). The TEM image (Figure 3c) of the neat sample indicates a lamellar morphology with a domain spacing of 15.5 nm. Surprisingly, well-defined lamellae are observed in the TEM image, which is in contrast with the broad peaks seen in the SAXS data. At temperatures above the melting point of P3EHT (90 and 120 °C), the SAXS scattering profiles show two distinct Bragg peaks at $\sqrt{6}q^*$ and $\sqrt{8}q^*$, consistent with the gyroid morphology. The characteristic domain spacing, d, is 12.3 nm. Further increase of the temperature to 125 °C leads to a disordered structure at a q_{max} of 0.51 nm^{-1}. In the inset of Figure 3a, a plot of the full width at half-maximum of q_{max} (fwhm) vs temperature shows a clear jump in fwhm, which is typical for an order-to-disorder phase transition (ODT). The ODT is reversible, as evidenced by the return of the gyroid morphology after the sample was cooled back down to 90 °C (Figure 3b). This is the first evidence of the existence of an ODT for a P3EHT-containing block copolymer.

We use the ODT to estimate the value of χ between P3EHT and PEO. There are currently no literature reports of statistical segment length of P3EHT chains in the melt state, l_{EHT}. We apply the random phase approximation to the SAXS data in the disordered state to obtain l_{EHT} as outlined by Lin et al. (refer to Supporting Infornmation).[31] In the mean-field theory the value of q_{max} depends on statistical segment lengths only and not on χ. Thus, knowing the literature value for the statistical segment length of PEO chains, l_{EO}, 0.72 nm,[32] and the value of q_{max} in the disordered state, 0.51 nm^{-1}, we obtain l_{EHT} = 1.1 nm. The statistical segment lengths and χ parameters in this work are

dx.doi.org/10.1021/nl302454c | Nano Lett. 2012, 12, 4901−4906

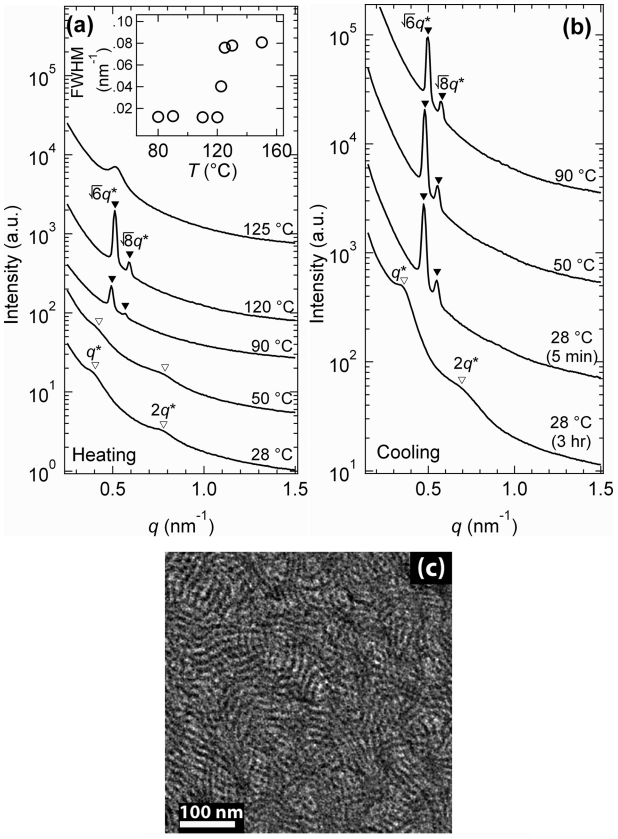

Figure 3. (a) Heating scan and (b) cooling scan SAXS curves of P3EHT-*b*-PEO (r = 0). The inset in (a) is the full width half-maximum (fwhm) of the primary scattering peak vs T (temperature) curve, indicating an order-to-disorder phase (ODT) transition. The melt-state gyroid morphology (90 °C) is destroyed ("breakout") upon crystallization of the P3EHT block at 28 °C. The filled triangles denote peaks corresponding to the gyroid morphology, and the unfilled triangles denote peaks corresponding to the lamellar morphology. (c) Bright-field transmission electron microscopy (TEM) image of P3EHT-*b*-PEO (r = 0) shows that the "breakout" morphology is lamellar at room temperature. Contrast arises from the higher electron density in the semicrystalline P3EHT (dark phase).

based on reference volume of 0.1 nm^3. Thus, the conformational asymmetry factor for our system is l_{EHT}/l_{EO} = 1.5. The mean-field phase diagram for block copolymer with l_{EHT}/l_{EO} = 1.5 and ϕ_{EHT} = 0.71 contains a transition from gyroid to cylinder at χN = 20, a transition to cylinders to spheres at χN = 14.5, and a transition from spheres to disordered at χN = 14.[33] However, only a gyroid to disorder transition was observed in our P3EHT-*b*-PEO (r = 0) at 125 °C. We thus conclude the value of χN for our system at 125 °C is between 14 and 20. Since N = 108, we conclude that 0.13 < χ < 0.19 at 125 °C. To our knowledge, this is the first quantitative measurement of χ between conventional polymers such as PEO and poly(3-alkylthiophene) chains. This is the first step toward prediction of the morphology of block copolymers containing poly(3-alkylthiophene) chains.

The above method for determining χ only applies to conventional block copolymers with Gaussian chains. P3EHT is, however, a semiflexible polymer.[10,34] Theoretical work on the phase behavior of semiflexible block copolymers shows that the value of χN at the ODT for these systems depends on magnitude of the Maier−Saupé parameter, μ, relative to χ.[35−38] The Maier−Saupé parameter quantifies interactions between rodlike molecules in the mean-field limit. The μ value for P3EHT is 0.01 at 125 °C;[34] thus, μ/χ is estimated to be between 0.052 and 0.076 for our system. The predictions in ref 35 indicate that such a small value of μ/χ has a negligible effect on the value of χN at the ODT. We note in passing that our estimate is based entirely on the mean-field theory of block copolymers; i.e., fluctuation corrections[39] are ignored.

In Figure 3b, we show the SAXS data for r = 0 during the cooling run after heating the P3EHT-*b*-PEO to 150 °C. Unlike the heating step to 50 °C where lamellar morphology was observed (Figure 3a), the cooling step to 50 °C shows retention of the gyroid morphology (Figure 3b). DSC data and WAXS experiments during cooling runs indicate that P3EHT does not recrystallize at 50 °C (data not shown). It is not clear if this observed suppression of crystallization at 50 °C is due to kinetic factors. Further cooling to 28 °C shows the gyroid morphology at early times and a lamellar morphology at long times (Figure 3b). This observation indicates that the crystallization of P3EHT block destroys the melt-state morphology. In other words, the P3EHT crystals "break out" of the confined domains dictated by thermodynamic segregation of the blocks (χN and ϕ_{EHT}). This is due to the nonglassy nature of the PEO block and the fact that χN is between 14 and 20; i.e., the system is weakly segregated. The fact that the breakout structure is lamellar is not completely unexpected as previous theories[23,24] and experiments[12−14,21] on weakly segregated semicrystalline block copolymers show the crystalline-state morphology is often lamellar regardless of the melt-state morphology.

Segregation between the blocks can be increased by the addition of LiTFSI salt to P3EHT-*b*-PEO. In Figure 4a, the SAXS profile of the P3EHT-*b*-PEO/LiTFSI mixture with r = 0.125 in the melt state (150 °C) shows the presence of the lamellar morphology indicated by the Bragg peaks at q^*, $2q^*$, $3q^*$, and $4q^*$ corresponding to a d of 15.4 nm. The sample was quenched to 28 °C to allow for the crystallization of P3EHT block. We see that the lamellar morphology is retained even after 12 h. However, the Bragg peaks broaden slightly and the lamellar spacing increases; d increases from 15.4 to 18.3 nm during the 12 h annealing step. The DSC and WAXS data shown in Figure 2 indicate that the P3EHT block in the P3EHT-*b*-PEO/LiTFSI mixture with r = 0.125 crystallizes on this time scale. We thus attribute the broadening the Bragg peaks to P3EHT crystallization. A lamellar morphology is also observed in the TEM image of the P3EHT-*b*-PEO/LiTFSI mixture with r = 0.125 shown in Figure 4b, where the characteristic domain spacing is 17.5 nm. It is evident that the P3EHT-*b*-PEO/LiTFSI mixture with r = 0.125 exhibits confined crystallization at room temperature. This is attributed to an increase in segregation, χN, and the fact that the melt-state morphology is lamellar. Extrapolation of the data for polystyrene-*b*-poly(ethylene oxide) (PS-*b*-PEO)/LiTFSI mixtures[41] shows that χ increases by a factor of about 7 when r is increased from 0 to 0.125. Assuming that the thermodynamics of PS-*b*-PEO/LiTFSI and P3EHT-*b*-PEO/LiTFSI systems are similar, we anticipate that χN is about 100 for P3EHT-*b*-PEO/LiTFSI mixture with r = 0.125. The DSC data in Figure 2 indicate that the P3EHT crystals melt in both r = 0 and r = 0.125 samples around 80 °C. In spite of this, the r = 0 sample crystallizes in 90 min while there is virtually no evidence of crystallization in the r = 0.125 sample after 90 min of annealing. The difference in crystallization kinetics can be attributed to confinement. The r = 0 sample exhibits breakout crystallization,

dx.doi.org/10.1021/nl302454c | *Nano Lett.* 2012, 12, 4901−4906

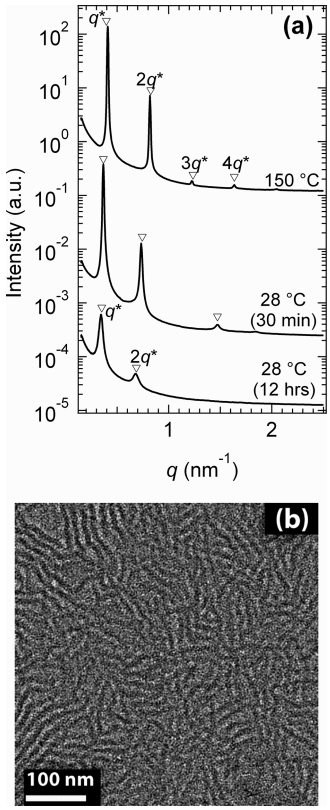

Figure 4. (a) Cooling run SAXS curves of P3EHT-*b*-PEO (r = 0.125). The lamellar morphology is retained after 12 h at 28 °C where P3EHT block fully crystallizes (confined crystallization). (c) Bright-field TEM image of P3EHT-*b*-PEO (r = 0.125) at room temperature indicating a lamellar morphology. Contrast arises from the higher electron density in the semicrystalline P3EHT (dark phase).

while r = 0.125 sample exhibits confined crystallization. Previous studies on semicrystalline block copolymers have shown that breakout crystallization follows sigmoidal kinetics, while confined crystallization follows first-order kinetics.[16,42,43] In particular, the crystallization half-time is more highly dependent on crystallization temperature during confined crystallization. As a result, varying the temperature for isothermal crystallization of the r = 0.125 sample could greatly affect the time needed to fully crystallize the P3EHT block. The magnitude in time difference for crystallization (hours) between r = 0 and r = 0.125 is far greater than previously reported confined/breakout crystallization behavior in block copolymers. This could be attributed to the inherent slower crystallization kinetics of P3EHT. Further work is needed to fully understand the crystallization kinetics in P3EHT-*b*-PEO during confinement and breakout.

In summary, a P3EHT-*b*-PEO copolymer was synthesized by producing ethynyl-terminated P3EHT in one step using GRIM polymerization followed by coupling to an azide-terminated PEO block through click chemistry. This facile approach may be used for synthesizing a variety of poly(3-alkylthiophene)-containing block copolymers. We have demonstrated that the morphology of this copolymer can be controlled by thermodynamic parameters such as temperature and segregation strength (χN). The segregation strength was adjusted by the addition of LiTFSI salt. In the melt state, the salt-free sample (r = 0) exhibits a gyroid morphology while the salt-containing sample (r = 0.125) exhibits a lamellar morphology. Quenching the salt-free sample to room temperature results in a lamellar morphology due to the breakout of the P3EHT crystals. In contrast, there is little change in the morphology of the salt-containing sample upon quenching to room temperature; i.e., we observed confined crystallization. This qualitative change is attributed to increase in χN from about 17 to 100. Finally, this work provides the first estimate for the value of χ between P3AT chains and conventional polymers such as PEO.

■ ASSOCIATED CONTENT

Ⓢ Supporting Information

Detailed synthetic procedures, salt sample preparation, scattering procedures, TEM procedure, and calculation of statistical segment length. This material is available free of charge via the Internet at http://pubs.acs.org.

■ AUTHOR INFORMATION

Corresponding Author

*E-mail nbalsara@berkeley.edu, Ph 510.642.8937, Fax 510.642.4778.

Author Contributions

⊥These authors contributed equally.

Notes

The authors declare no competing financial interest.

■ ACKNOWLEDGMENTS

The polymer synthesis was supported the BATT program at Lawrence Berkeley National Laboratory (LBNL), U.S. DOE Contract DE-AC02-05CH11231. The polymer characterization portion was supported by a grant from the National Science Foundation (CBET 0966632). SAXS experiments were performed at the LBNL Advanced Light Source, under the same contract, while WAXS experiments were performed at the Stanford Synchrotron Radiation Laboratory. Electron microscopy work was supported by the Electron Microscopy of Soft Matter Program at LBNL supported by the Director, Office of Science, Office of Basic Energy Sciences, Materials Sciences and Engineering Division, of the U.S. Department of Energy under Contract No.DE-AC02-05CH11231. We thank B. McCulloch for helpful discussions.

■ REFERENCES

(1) Segalman, R. A.; McCulloch, B.; Kirmayer, S.; Urban, J. J. *Macromolecules* **2009**, *42* (23), 9205−9216.
(2) Steele, B. C. H.; Heinzel, A. *Nature* **2001**, *414* (6861), 345−352.
(3) Tarascon, J. M.; Armand, M. *Nature* **2001**, *414* (6861), 359−367.
(4) Darling, S. B. *Energy Environ. Sci.* **2009**, *2* (12), 1266−1273.
(5) Sauve, G.; McCullough, R. D. *Adv. Mater.* **2007**, *19* (14), 1822−1825.
(6) Iovu, M. C.; Zhang, R.; Cooper, J. R.; Smilgies, D. M.; Javier, A. E.; Sheina, E. E.; Kowalewski, T.; McCullough, R. D. *Macromol. Rapid Commun.* **2007**, *28* (17), 1816−1824.
(7) Iovu, M. C.; Jeffries-El, M.; Zhang, R.; Kowalewski, T.; Mccullough, R. D. *J. Macromol. Sci. A* **2006**, *43* (12), 1991−2000.
(8) Craley, C. R.; Zhang, R.; Kowalewski, T.; McCullough, R. D.; Stefan, M. C. *Macromol. Rapid Commun.* **2009**, *30* (1), 11−16.
(9) Matsen, M. W.; Bates, F. S. *Macromolecules* **1996**, *29* (4), 1091−1098.
(10) Ho, V.; Boudouris, B. W.; McCulloch, B. L.; Shuttle, C. G.; Burkhardt, M.; Chabinyc, M. L.; Segalman, R. A. *J. Am. Chem. Soc.* **2011**, *133* (24), 9270−9273.
(11) Moon, H. C.; Bae, D.; Kim, J. K. *Macromolecules* **2012**, *45* (12), 5201−5207.

(12) Rangarajan, P.; Register, R. A.; Fetters, L. J.; Bras, W.; Naylor, S.; Ryan, A. J. *Macromolecules* **1995**, *28* (14), 4932−4938.
(13) Ryan, A. J.; Hamley, I. W.; Bras, W.; Bates, F. S. *Macromolecules* **1995**, *28* (11), 3860−3868.
(14) Quiram, D. J.; Register, R. A.; Marchand, G. R. *Macromolecules* **1997**, *30* (16), 4551−4558.
(15) Hamley, I. W. *Adv. Polym. Sci.* **1999**, *148*, 113−137.
(16) Loo, Y. L.; Register, R. A.; Ryan, A. J. *Phys. Rev. Lett.* **2000**, *84* (18), 4120−4123.
(17) Loo, Y. L.; Register, R. A.; Ryan, A. J.; Dee, G. T. *Macromolecules* **2001**, *34* (26), 8968−8977.
(18) Loo, Y. L.; Register, R. A.; Ryan, A. J. *Macromolecules* **2002**, *35* (6), 2365−2374.
(19) Zhu, L.; Cheng, S. Z. D.; Calhoun, B. H.; Ge, Q.; Quirk, R. P.; Thomas, E. L.; Hsiao, B. S.; Yeh, F.; Lotz, B. *Polymer* **2001**, *42* (13), 5829−5839.
(20) Xu, J. T.; Fairclough, J. P. A.; Mai, S. M.; Chaibundit, C.; Mingvanish, M.; Booth, C.; Ryan, A. J. *Polymer* **2003**, *44* (22), 6843−6850.
(21) Mai, S. M.; Fairclough, J. P. A.; Viras, K.; Gorry, P. A.; Hamley, I. W.; Ryan, A. J.; Booth, C. *Macromolecules* **1997**, *30* (26), 8392−8400.
(22) Hamley, I. W.; Fairclough, J. P. A.; Bates, F. S.; Ryan, A. J. *Polymer* **1998**, *39* (6−7), 1429−1437.
(23) Dimarzio, E. A.; Guttman, C. M.; Hoffman, J. D. *Macromolecules* **1980**, *13* (5), 1194−1198.
(24) Whitmore, M. D.; Noolandi, J. *Macromolecules* **1988**, *21* (5), 1482−1496.
(25) Chang, J.-F.; Sun, B.; Breiby, D. W.; Nielsen, M. M.; Sölling, T. I.; Giles, M.; McCulloch, I.; Sirringhaus, H. *Chem. Mater.* **2004**, *16* (23), 4772−4776.
(26) Sirringhaus, H.; Brown, P. J.; Friend, R. H.; Nielsen, M. M.; Bechgaard, K.; Langeveld-Voss, B. M. W.; Spiering, A. J. H.; Janssen, R. A. J.; Meijer, E. W.; Herwig, P.; de Leeuw, D. M. *Nature* **1999**, *401* (6754), 685−688.
(27) Ho, V.; Boudouris, B. W.; Segalman, R. A. *Macromolecules* **2010**, *43* (19), 7895−7899.
(28) Boudouris, B. W.; Ho, V.; Jimison, L. H.; Toney, M. F.; Salleo, A.; Segalman, R. A. *Macromolecules* **2011**, *44* (17), 6653−6658.
(29) Javier, A. E.; Patel, S. N.; Hallinan, D. T.; Srinivasan, V.; Balsara, N. P. *Angew. Chem., Int. Ed.* **2011**, *50* (42), 9848−9851.
(30) Patel, S. N.; Javier, A. E.; Stone, G. M.; Mullin, S. A.; Balsara, N. P. *ACS Nano* **2012**, *6* (2), 1589−1600.
(31) Lin, C. C.; Jonnalagadda, S. V.; Kesani, P. K.; Dai, H. J.; Balsara, N. P. *Macromolecules* **1994**, *27* (26), 7769−7780.
(32) Eitouni, H. B.; Balsara, N. P. Thermodynamics of Polymer Blends. In *Physical Properties of Polymers Handbook*; Mark, J. E., Ed.; Springer: New York, 2007; pp 339−356.
(33) Matsen, M. W.; Bates, F. S. *J. Polym. Sci., Polym. Phys.* **1997**, *35* (6), 945−952.
(34) Ho, V.; McCulloch, B.; Segalman, R., personal correspondence.
(35) Singh, C.; Goulian, M.; Liu, A. J.; Fredrickson, G. H. *Macromolecules* **1994**, *27* (11), 2974−2986.
(36) Hammouda, B. *J. Chem. Phys.* **1993**, *98* (4), 3439−3444.
(37) Holyst, R.; Schick, M. *J. Chem. Phys.* **1992**, *96* (1), 730−740.
(38) Pryamitsyn, V.; Ganesan, V. *J. Chem. Phys.* **2004**, *120* (12), 5824−5838.
(39) Fredrickson, G. H.; Helfand, E. *J. Chem. Phys.* **1987**, *87* (1), 697−705.
(40) Nojima, S.; Ono, M.; Ashida, T. *Polym. J.* **1992**, *24* (11), 1271−1280.
(41) Wanakule, N. S.; Virgili, J. M.; Teran, A. A.; Wang, Z. G.; Balsara, N. P. *Macromolecules* **2010**, *43* (19), 8282−8289.
(42) Xu, J. T.; Fairclough, J. P. A.; Mai, S. M.; Ryan, A. J.; Chaibundit, C. *Macromolecules* **2002**, *35* (18), 6937−6945.
(43) Xu, J. T.; Turner, S. C.; Fairclough, J. P. A.; Mai, S. M.; Ryan, A. J.; Chaibundit, C.; Booth, C. *Macromolecules* **2002**, *35* (9), 3614−3621.